Entrainment control in a noisy neural system

Diek W. Wheeler* and W. C. Schieve†

Center for Studies in Statistical Mechanics and Complex Systems, Physics Department, The University of Texas, Austin, Texas 78712

(Received 24 January 2002; revised manuscript received 10 December 2002; published 25 April 2003)

The open-plus-closed-loop (OPCL) entrainment control put forth by Jackson and Grosu [Physica D **85**, 1 (1995)] is applied to an effective-neuron system as a way to extract stable limit cycles from a chaotic attractor, analogous to the retrieval of memories from a memory searching state. Additive Gaussian white noise, representing the natural noise inherent in any real dynamical system, is added to the entrainment control mechanism. Moderate levels of additive noise have little effect on successful entrainment, as reflected in phase-space plots and Lyapunov exponents. All three Lyapunov exponents are negative, which suggests parallels between OPCL control and chaotic synchronization.

DOI: 10.1103/PhysRevE.67.046219 PACS number(s): 05.45.Gg, 02.50.Ey, 05.45.Pq

I. INTRODUCTION

In the 1990s there were literally hundreds of papers published on the control of chaos in nonlinear systems. Reasonably complete overviews of chaos control techniques can be found in Chen and Dong [1] and Boccaletti *et al.* [2].

One such control mechanism is entrainment control, of which there are many variations. Here we discuss a method which is based on the work first suggested by Hübler [3] and has since found many applications [4–10]. Jackson and Grosu [11] extended Hübler's original control into an open-plus-closed-loop (OPCL) control scheme, so that it became applicable to most systems. Since its inception, the OPCL control method has been expanded upon both theoretically [12–20] and experimentally [21–23].

OPCL control has some major strengths over other control methods such as the parameter feedback mechanism of Ott, Grebogi, and Yorke [24]. OPCL does not require access to the system parameters, and the goal dynamics are not limited to unstable periodic orbits. OPCL control does, however, require a good model of the system dynamics for it to function properly.

The system model emphasized in this work is an effective-neuron system exhibiting chaotic dynamics described by Wheeler and Schieve [25]. Even before the discovery of chaotic dynamics within brain activity in 1985 [26–29], many proposals were made as to the nature and function of such dynamics. It has been suggested by Skarda and Freeman [30,31] and Tsuda, Koerner, and Shimizu [32] that chaos allows a neural system to quickly search through and retrieve all stored attractors, or memories. Entrainment control is investigated as a possible mechanism for such recall. Here we also examine how additive noise affects OPCL control, since noise is a natural part of any biological system.

Section II reviews the theoretical basis for OPCL entrainment control. The application of OPCL control to an effective-neuron system and the extent of the basin of entrainment are discussed in Sec. III. Section IV covers the introduction of noise to the OPCL control process, examining the effects of additive noise on the transition from a chaotic attractor to a stable limit cycle. Concluding remarks are presented in Sec. V.

*Present address: Department of Neurobiology, University of Pittsburgh School of Medicine, Pittsburgh, PA 15261.

†Corresponding author. FAX: (512) 471-9637. Email: FSchieve@aol.com.

II. ENTRAINMENT CONTROL

In entrainment control, the objective is to entrain a system,

$$\frac{dx}{dt}=F(x,t), \tag{1}$$

to a desired goal dynamics $g(t)$ so that

$$\lim_{t\to\infty}[x(t)-g(t)]=0. \tag{2}$$

As this method of control was originally conceived, $g(t)$ would satisfy

$$\frac{dg}{dt}=F(g,t), \tag{3}$$

which could be any type of desired motion within the system.

In order to satisfy Eq. (2), the equation

$$\frac{dx}{dt}=F(x,t)+S(t)\left[\frac{dg}{dt}-F(g,t)\right] \tag{4}$$

must be met, where $S(t)$ is a switching function added to ease violent transitions [7]. The portion in brackets is to be satisfied at all times, as originally proposed by Hübler and Lüscher [4].

The difficulty with this control method, as it stands, is that it is hard to determine the extent of the basin of entrainment for an arbitrary $g(t)$. If the goal dynamics $g(t)$ do not overlap the basin of entrainment of the experimental dynamics $x(t)$, then Eq. (2) will not be satisfied.

Jackson and Grosu [11] proposed a modification of this entrainment control mechanism that expands the basin of entrainment to include the entire phase space for any $g(t)$. The goal dynamics $g(t)$ can now describe any system,

$$\frac{dg}{dt}=G(g,t), \tag{5}$$

and can be independent of the experimental system. Jackson and Grosu's more general solution to Eq. (4) is

$$\frac{dx}{dt}=F(x,t)+S(t)\left[\frac{dg}{dt}-F(g,t)+\left(\frac{\partial F(g,t)}{\partial g}-A\right)(g-x)\right], \tag{6}$$

where A is a constant matrix with eigenvalues that all have negative real parts.

Chen [33] independently suggested adding a term to Eq. (4), however, the extended control of Jackson and Grosu [11] is stronger, as it contains not only a control matrix but also a partial-derivative term, which ensures that Eq. (2) is satisfied. The necessity of this term can be shown by examining the stability of a small perturbation introduced into the system equations. Set $x=g+u$, where $u \ll 1$. This leads to

$$\frac{du}{dt}=F(g+u,t)-F(g,t)-C(g,t)u. \tag{7}$$

If $F(g+u,t)$ is expanded to first order about the perturbation u, then

$$\frac{du}{dt}=\frac{\partial F(g,t)}{\partial g}u-C(g,t)u=Au. \tag{8}$$

Since the eigenvalues of matrix A all have negative real parts, Eq. (2) is satisfied. Therefore, OPCL control establishes a finite basin of entrainment for the goal dynamics. With this in mind, the following section will explore the implementation of entrainment control in a chaotic neural system.

III. ENTRAINMENT CONTROL IN AN EFFECTIVE-NEURON SYSTEM

The general entrainment control of Eq. (6) is now applied to the effective-neuron system originally explored by Wheeler and Schieve [25],

$$\dot{U}_1=U_2, \tag{9}$$

$$\dot{U}_2=-\frac{\eta_1}{M_1}U_2-\frac{K_1}{M_1}U_1+\frac{J_{11}}{M_1}\tanh(U_1)+\frac{J_{13}}{M_1}\tanh(U_3), \tag{10}$$

$$\dot{U}_3=-\frac{K_3}{\eta_3}U_3+\frac{J_{31}}{\eta_3}\tanh(U_1)+\frac{J_{33}}{\eta_3}\tanh(U_3), \tag{11}$$

where U is the neural potential, η is the capacitance, K is the conductance, M is the inertia/inductance, and J is the weight matrix for the network. This system is derived from the base two-neuron system explored by Zeng, Schieve, and Das [34], Kwek and Li [35], and Beer [36]. The inertia/inductance is added to provide oscillatory and resonant behavior, as well as complexity. Biological support for this inertial term comes from instances where a neuron's behavior can be described as if its equivalent circuit model possessed a phenomenological inductance (Cole and Baker [37]; Hodgkin and Huxley [38]; Detwiler, Hodgkin, and McNaughton [39]). Further examples of phenomenological inductance can be found in Wheeler and Schieve [25] and Wheeler [40]. The parameter M has no effect on the locations of the fixed points in phase space, but it does influence the dynamic stability of the fixed points. Using M as a bifurcation parameter, the system can make transitions from period doubling to chaos. Figure 1 shows an example of how entrainment control can be used in this system. A chaotic attractor from the effective-neuron system is entrained to a period-two limit cycle, which also exists within the neural system [25].

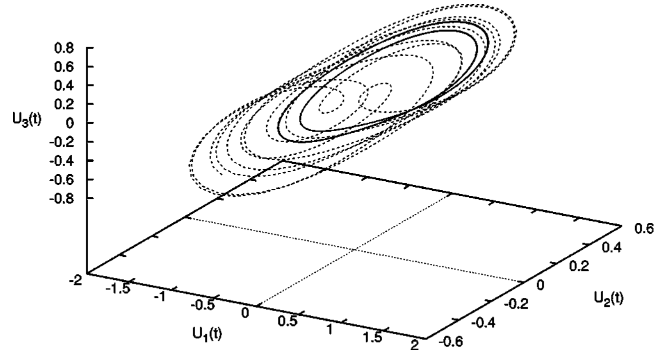

FIG. 1. Deterministic entrainment control in an effective-neuron system. A chaotic attractor ($M=2.5$) is entrained to a stable period-two limit cycle ($M=2.0$), where both attractors exist within the same system. Control-matrix coefficients $a_{ii}=-1$.

A. Basin of entrainment

The extent of the basin of entrainment is used to evaluate the efficacy of entrainment control in the effective-neuron system. This is accomplished by examining the stability of a perturbation introduced into the system equations. Setting $U_x=U_g+U_\epsilon$, where $U_\epsilon \ll 1$, and expanding $F(U_g+U_\epsilon,t)$ about the perturbation leads to

$$\frac{dU_\epsilon}{dt}=AU_\epsilon+\frac{1}{2}\frac{\partial^2 F(U_g,t)}{\partial U_g^2}U_\epsilon^2+\frac{1}{6}\frac{\partial^3 F(U_g,t)}{\partial U_g^3}U_\epsilon^3+\cdots. \tag{12}$$

Since the eigenvalues of A all have negative real parts, first-order solutions for the perturbation U_ϵ have the form $U_\epsilon = U_\epsilon^0 \exp(at)$ and vanish at large values of t. Applying Eq. (12) to the effective-neuron system results in

$$\frac{dU_{1\epsilon}}{dt}=a_{11}U_{1\epsilon}, \tag{13}$$

$$\frac{dU_{2\epsilon}}{dt}=a_{22}U_{2\epsilon}+\frac{J_{11}}{M_1}\bigg[-\text{sech}^2(U_{1g})\tanh(U_{1g})U_{1\epsilon}^2 +\frac{1}{6}\text{sech}^2(U_{1g})[4\tanh^2(U_{1g})+\text{sech}^2(U_{1g})]U_{1\epsilon}^3 +\cdots\bigg]+\frac{J_{13}}{M_1}\bigg[-\text{sech}^2(U_{3g})\tanh(U_{3g})U_{3\epsilon}^2 +\frac{1}{6}\text{sech}^2(U_{3g})[4\tanh^2(U_{3g}) +\text{sech}^2(U_{3g})]U_{3\epsilon}^3+\cdots\bigg], \tag{14}$$

$$\frac{dU_{3\epsilon}}{dt}=a_{33}U_{3\epsilon}+\frac{J_{31}}{\eta_3}\bigg[-\text{sech}^2(U_{1g})\tanh(U_{1g})U_{1\epsilon}^2 +\frac{1}{6}\text{sech}^2(U_{1g})[4\tanh^2(U_{1g})+\text{sech}^2(U_{1g})]U_{1\epsilon}^3 +\cdots\bigg]+\frac{J_{33}}{\eta_3}\bigg[-\text{sech}^2(U_{3g})\tanh(U_{3g})U_{3\epsilon}^2 +\frac{1}{6}\text{sech}^2(U_{3g})[4\tanh^2(U_{3g}) +\text{sech}^2(U_{3g})]U_{3\epsilon}^3+\cdots\bigg]. \tag{15}$$

Since the first-order perturbation solutions vanish, the stability of the system is therefore determined by the remaining terms. The higher-order terms in Eqs. (14) and (15) consist of powers of $\tanh(U_g)$, $\text{sech}(U_g)$, $U_{1\epsilon}$, and $U_{3\epsilon}$. The $\tanh(U_g)$ terms are bound between -1 and $+1$, and the $\text{sech}(U_g)$ terms are bound between 0 and $+1$. The solutions to $U_{1\epsilon}$ are known, $U_{1\epsilon}=U_{1\epsilon}^0\exp(a_{11}t)$, so all of the terms containing powers of $U_{1\epsilon}$ can be made to damp out arbitrarily quickly. If $U_{3\epsilon}$ is selected so that it is bound by the exponential $C_3\exp(\lambda_3 t)$, then inserting this solution into Eq. (15) results in

$$\lambda_3C_3=a_{33}C_3+[(\cdots)e^{(2a_{11}-\lambda_3)t}+(\cdots)e^{(3a_{11}-\lambda_3)t}+\cdots] +[(\cdots)e^{\lambda_3 t}+(\cdots)e^{2\lambda_3 t}+\cdots], \tag{16}$$

where the ellipses in parentheses have been used to reduce clutter in the equation. If λ_3 is chosen such that $2a_{11}-\lambda_3<0$ and $\lambda_3<0$, then in the limit as $t\to\infty$, $\lambda_3\to a_{33}<0$. A similar approach can be used for Eq. (14), which yields

$$\lambda_2C_2=a_{22}C_2+[(\cdots)e^{(2a_{11}-\lambda_2)t}+(\cdots)e^{(3a_{11}-\lambda_2)t}+\cdots] +[(\cdots)e^{(2\lambda_3-\lambda_2)t}+(\cdots)e^{(3\lambda_3-\lambda_2)t}+\cdots]. \tag{17}$$

By selecting λ_2 so that $2a_{11}-\lambda_2<0$ and $2\lambda_3-\lambda_2<0$, then as $t\to\infty$, $\lambda_2\to a_{22}<0$. To summarize, the basin of entrainment for the effective-neuron system is not restricted by $U_g(t)$ as long as the following inequalities are satisfied:

$$2a_{11}<a_{22}<0, \tag{18}$$

$$4a_{11}<2a_{33}<a_{22}<0. \tag{19}$$

B. Criteria for entrainment control

The entrainment-control equations specific to the effective-neuron system are

$$\frac{dU_{1x}}{dt}=U_{2x}+S(t)\left[\frac{dU_{1g}}{dt}-U_{2x}-a_{11}(U_{1g}-U_{1x})\right], \tag{20}$$

$$\frac{dU_{2x}}{dt}=-\frac{\eta_1}{M_1}U_{2x}-\frac{K_1}{M_1}U_{1x}+\frac{J_{11}}{M_1}\tanh(U_{1x}) +\frac{J_{13}}{M_1}\tanh(U_{3x})+S(t)\bigg[\frac{dU_{2g}}{dt}+\frac{\eta_1}{M_1}U_{2x}+\frac{K_1}{M_1}U_{1x} +\frac{J_{11}}{M_1}[(U_{1g}-U_{1x})\text{sech}^2(U_{1g})-\tanh(U_{1g})] +\frac{J_{13}}{M_1}[(U_{3g}-U_{3x})\text{sech}^2(U_{3g})-\tanh(U_{3g})] -a_{22}(U_{2g}-U_{2x})\bigg], \tag{21}$$

$$\frac{dU_{3x}}{dt}=-\frac{K_3}{\eta_3}U_{3x}+\frac{J_{31}}{\eta_3}\tanh(U_{1x})+\frac{J_{33}}{\eta_3}\tanh(U_{3x})+S(t) \times\bigg[\frac{dU_{3g}}{dt}+\frac{K_3}{\eta_3}U_{3x} +\frac{J_{31}}{\eta_3}[(U_{1g}-U_{1x})\text{sech}^2(U_{1g})-\tanh(U_{1g})] +\frac{J_{33}}{\eta_3}[(U_{3g}-U_{3x})\text{sech}^2(U_{3g})-\tanh(U_{3g})] -a_{33}(U_{3g}-U_{3x})\bigg]. \tag{22}$$

Jackson and Grosu's [11] added control mechanism,

$$C=\left|\frac{\partial F(U_g,t)}{\partial U_g}-A\right|, \tag{23}$$

results in a cubic equation that can be solved for the eigenvalues λ.

To insure that the eigenvalues of the matrix $C(U_g,t)$ have negative real parts, the Routh-Hurwitz stability criteria must be met. Given the following general cubic equation to be solved for the eigenvalues of $C(U_g,t)$,

$$\lambda^3+b_1\lambda^2+b_2\lambda+b_3=0, \tag{24}$$

the eigenvalues will all have negative real parts if the following three criteria are satisfied:

$$b_1>0, \tag{25}$$

$$b_3>0, \tag{26}$$

$$b_1b_2-b_3>0. \tag{27}$$

Since the Routh-Hurwitz criteria are inequalities, it is proper to maximize the terms in the equation before they are evaluated. This means setting the $\operatorname{sech}(U_g)$ terms to one. Also, to be practical, specific values for the various parameters are assigned, $K_1=K_3=\eta_1=\eta_3=1$. As a final evaluative simplification, all three A-matrix coefficients are assumed to be the same $(=a_{11})$. The stability criteria are now

$$b_1=\frac{1}{M_1}+1-J_{33}-3a_{11}>0, \tag{28}$$

$$b_3=\frac{1}{M_1}-\frac{J_{11}}{M_1}-\frac{J_{33}}{M_1}+\frac{J_{11}J_{33}}{M_1}+\frac{J_{13}J_{31}}{M_1}+\left(\frac{J_{33}}{M_1}+\frac{J_{11}}{M_1}-\frac{2}{M_1}\right)a_{11}+\left(1-J_{33}+\frac{1}{M_1}\right)a_{11}^2-a_{11}^3>0, \tag{29}$$

$$b_1b_2-b_3=\left[\frac{1}{M_1}+1-J_{33}-3a_{11}\right]\left[\frac{2}{M_1}-\frac{J_{11}}{M_1}-\frac{J_{33}}{M_1}+\left(2J_{33}-\frac{2}{M_1}-2\right)a_{11}+3a_{11}^2\right]-\left[\frac{1}{M_1}-\frac{J_{11}}{M_1}-\frac{J_{33}}{M_1}+\frac{J_{11}J_{33}}{M_1}+\frac{J_{13}J_{31}}{M_1}+\left(\frac{J_{33}}{M_1}+\frac{J_{11}}{M_1}-\frac{2}{M_1}\right)a_{11}+\left(1-J_{33}+\frac{1}{M_1}\right)a_{11}^2-a_{11}^3\right]>0. \tag{30}$$

As an initial approximation, the first criterion is used to evaluate a_{11},

$$a_{11}<-\frac{1}{3}\left[\frac{1}{M_1}+1-J_{33}\right]. \tag{31}$$

By inserting the values $M_1=2.5$ and $J_{33}=1.44$, which have been demonstrated to yield chaotic behavior by Wheeler and Schieve [25], the inequality becomes

$$a_{11}<-\frac{1}{3}\left[\frac{1}{2.5}+1-1.44\right]=-0.04. \tag{32}$$

Therefore, given Eq. (32), which satisfies Eqs. (18) and (19), it is reasonable to select nearly any negative number for a_{11} to achieve full entrainment control. The only caveat is if one chooses a value of a_{11} that lies close to the inequality boundary. This may result in the basin of entrainment being reduced and Eq. (2) not being satisfied. To avoid such an occurrence, a_{11} should be selected so that $a_{11}\ll -0.04$.

IV. NOISY ENTRAINMENT CONTROL

Noise is inherent in any biological system, therefore, the OPCL control technique is modified to include additive noise. One of the keys to implementing the control method lies in the eigenvalues of the control-matrix A. Under noisy control, matrix A is replaced with matrix $N(t)$, the coefficients of which are produced by adding Gaussian white noise with zero mean and unit variance to the coefficients of matrix A.

The form of the switching function $S(t)$ used in these simulations is

$$S(t)=1-e^{-\lambda(t-t_{ON})}, \tag{33}$$

where t_{ON} is the time step value at which the switching function activates and $\lambda=0.1$ for all of the simulations.

A. Noise as a control mechanism

Skarda and Freeman [30,31] and Tsuda, Koerner, and Shimizu [32] have suggested that chaos in brain dynamics would allow for the rapid search and retrieval of stored memories. Several groups have specifically looked at the stabilization effects of noise in both real and model neural systems. Freeman *et al.* [41] looked at noise in a model of the olfactory bulb. In biologically-realistic solutions to their model, they were able to stabilize the chaotic dynamics of the system by adding low levels of noise. Rajasekar and Lakshmanan [42] looked at the effects of Gaussian noise on chaos in a Bonhoeffer–van der Pol oscillator. They discovered that for a critical noise level, the maximal Lyapunov exponent becomes negative, and the system loses its sensitive dependence on initial conditions. Wang [43] explored the effects of a dynamical environment on model neural networks. He described how varying the noise level with time can induce transitions from ordered states to chaotic states, and vice versa. He proposed that such a varying environment might facilitate information processing, such as memory retrieval. Whereas the above groups examined the use of noise as a control mechanism unto itself, we investigate the effects of adding noise to an already established deterministic control mechanism.

B. Entrainment from a chaotic attractor

Here we discuss a chaotic attractor entrained to a period-two limit cycle. Both attractors exist within the effective-neuron system described previously in Sec. III [Eqs. (9)–(11)], with $K_1=K_3=\eta_1=\eta_3=1$ and

$$J=\begin{vmatrix} 0.43 & 1.50 \\ -0.25 & 1.44 \end{vmatrix}. \tag{34}$$

The chaotic attractor occurs at $M=2.5$, and the limit cycle appears at $M=2.0$. The entrainment equations are same as Eqs. (20)–(22) from Sec. III, except the a_{ii} terms have been replaced by their stochastic counterparts, $n_{ii}(t)=-1+noise$. To reiterate, the concept being explored is the ability of the neural system to use the chaotic attractor to search through its memory space, in the presence of noise, until the system finally entrains to a desired memory [30–32].

The lower limit for the noise amplitude (10^{-5}) was determined by the accuracy of the Lyapunov exponent calculations, which were halted when all three exponents were stable to five decimal places. The upper limit (10^{-2}) was

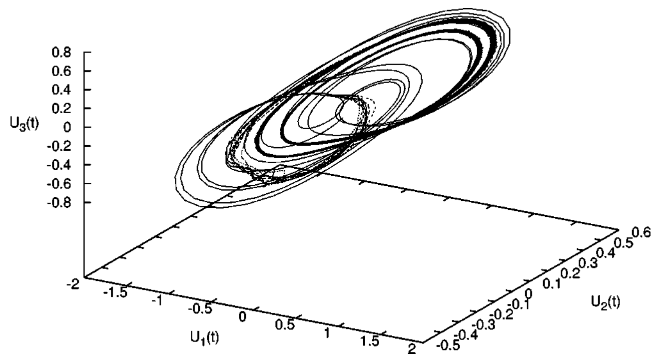

FIG. 2. Stochastic entrainment control in an effective-neuron system. Ten iterations of a chaotic attractor ($M=2.5$) are stochastically entrained to a period-two limit cycle ($M=2.0$). Despite the divergence of the phase-space paths from one another due to added noise, eventually all ten paths become entrained to the limit cycle. Control-matrix coefficients $a_{ii}=-1$ with an added noise level of 10^{-2}.

kept roughly two orders of magnitude below the amplitude of the normal phase-space displacement of the system dynamics. The Lyapunov exponents were calculated using the method of Wolf *et al.* [44]. The deterministic equations were numerically integrated with a fourth-order Runge-Kutta algorithm [45], and the stochastic equations were integrated with a second-order Runge-Kutta algorithm [46].

Figure 2 shows ten iterations of the noisy entrainment dynamics for an added noise level of 10^{-2}. Once the entrainment mechanism is activated, the phase-space paths for the different iterations begin to diverge. Despite this divergence, when the paths approach the limit cycle, they begin to reconverge.

The Lyapunov exponents are -1.40×10^{-3}, -79.70×10^{-3}, and -81.95×10^{-3} for the deterministically entrained system. Entrainment with increasing levels of noise causes the average first Lyapunov exponent to drift toward less negative values, as depicted in Fig. 3(a). Each point in the plot represents one thousand iterations of the stochastic dynamics, and the error bars depict one standard deviation from the averages. Overall, it appears that the presence of noise in the dynamics has little effect. The changes in the second and third Lyapunov exponents are depicted in Figs. 3(b) and 3(c). Again, there is a slight deviation in the exponents from the deterministic values as the noise level is increased, but the absolute magnitudes of the exponents remain fairly small and negative.

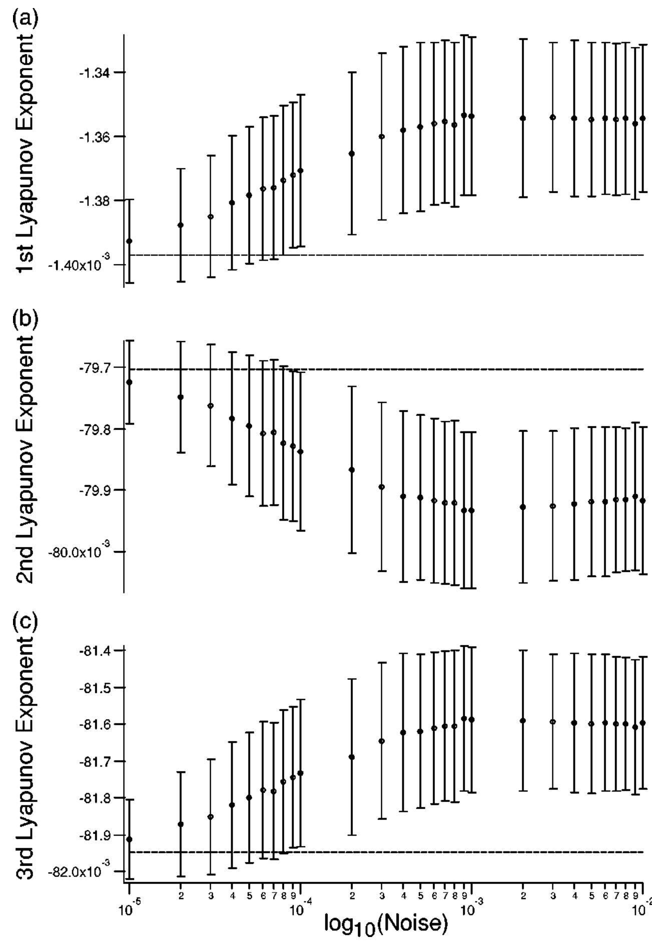

FIG. 3. Average Lyapunov exponents during stochatic entrainment (as in Fig. 2) for noise levels ranging from 10^{-5} to 10^{-2}. The horizontal dotted lines represent the deterministic values for the (a) first (-1.40×10^{-3}), (b) second (-79.70×10^{-3}), and (c) third (-81.95×10^{-3}) Lyapunov exponents. The average exponents deviate only slightly from the deterministic values. Each data point represents the average Lyapunov exponent after 1000 iterations of a chaotic attractor ($M=2.5$) being stochastically entrained to a period-two limit cycle ($M=2.0$). The error bars represent one standard deviation around the ensemble average.

V. CONCLUSION

The OPCL entrainment control method developed by Jackson and Grosu [11] can be modified by additive Gaussian white noise. This noisy entrainment control, when applied to an effective-neuron system, provides a robust way to extract stable limit cycles from a chaotic attractor, in analogy to a memory being recalled from a memory-searching state [30–32].

Noise is present in any real dynamical system, and the central nervous system is no exception. Therefore, noise is added to the entrained neural system to represent a low-level background that may originate as stray signals from various parts of the nervous system at large. The moderate levels of noise added to the OPCL control mechanism have little effect on the stability of the entrained attractors. This is reflected in phase-space plots and moderate changes in the average values of the Lyapunov exponents.

The fact that all three Lyapunov exponents are negative is suggestive of a synchronization criterion put forth by Pecora and Carroll [47,48]. The conditional Lyapunov exponents must be negative to successfully synchronize chaotic systems [47,48]. Grosu [13] and Chen and Liu [20] have previously applied OPCL control to synchronize chaotic systems, and Grosu described the mechanism as being robust in the presence of additive noise. Toral *et al.* [49] recently concluded that noise can aid in chaotic synchronization. Our results, however, correspond more with Grosu's than with Toral *et al.*'s, although we have made a more quantitative analysis of the effects of noise on OPCL control.

Our application of OPCL control to the effective-neuron system also differs from traditional chaotic synchronization [47,48] because we are not using a chaotic attractor as a driving signal. In our neural system, the period-two limit cycle drives the behavior of the chaotic attractor, so that the memory state drives the response of the search state into synchrony.

ACKNOWLEDGMENTS

D. W. W. was partially supported by the U.S. Department of Energy Grant No. DE-FG03-94ER14465. D.W.W. would like to thank G. A. Herin for helpful discussions.

[1] G. Chen and X. Dong, *From Chaos to Order: Methodologies, Perspectives and Applications* (World Scientific, Singapore, 1998).
[2] S. Boccaletti, C. Grebogi, Y.-C. Lai, H. Mancini, and D. Maza, Phys. Rep. **329**, 103 (2000).
[3] A. Hübler, Helv. Phys. Acta **62**, 343 (1989).
[4] A. Hübler and E. Lüscher, Naturwissenschaften **76**, 67 (1989).
[5] E. Lüscher and A. Hübler, Helv. Phys. Acta **62**, 544 (1989).
[6] E.A. Jackson, Phys. Lett. A **151**, 478 (1990).
[7] E.A. Jackson, Phys. Rev. A **44**, 4839 (1991).
[8] E.A. Jackson, Physica D **50**, 341 (1991).
[9] E.A. Jackson and A. Hübler, Physica D **44**, 407 (1990).
[10] E.A. Jackson and A. Kodogeorgiou, Physica D **44**, 253 (1992).
[11] E.A. Jackson and I. Grosu, Physica D **85**, 1 (1995).
[12] E.A. Jackson, Int. J. Bifurcation Chaos Appl. Sci. Eng. **5**, 1255 (1995).
[13] I. Grosu, Phys. Rev. E **56**, 1 (1997).
[14] L. Zonghua and C. Shigang, Phys. Rev. E **55**, 199 (1997).
[15] L.-Q. Chen and Y.-Z. Liu, Phys. Lett. A **245**, 87 (1998).
[16] L.-Q. Chen and Y.-Z. Liu, Phys. Lett. A **262**, 350 (1999).
[17] J. Wang and X. Wang, Int. J. Control **72**, 911 (1999).
[18] Y.-C. Tian, M.O. Tadé, and J. Tang, Chaos, Solitons Fractals **11**, 1029 (2000).
[19] L.-Q. Chen, Phys. Lett. A **281**, 327 (2001).
[20] L.-Q. Chen and Y.-Z. Liu, Int. J. Bifurcation Chaos Appl. Sci. Eng. **12**, 1219 (2002).
[21] E.A. Jackson and I. Grosu, Int. J. Bifurcation Chaos Appl. Sci. Eng. **5**, 1767 (1995).
[22] E.A. Jackson, Chaos **7**, 550 (1997).
[23] R. Weigel and E.A. Jackson, Int. J. Bifurcation Chaos Appl. Sci. Eng. **8**, 173 (1998).
[24] E. Ott, C. Grebogi, and J.A. Yorke, Phys. Rev. Lett. **64**, 1196 (1990).
[25] D.W. Wheeler and W.C. Schieve, Physica D **105**, 267 (1997).
[26] A. Babloyantz, C. Nicolis, and M. Salazar, Phys. Lett. A **111**, 152 (1985).
[27] J. Röschke and E. Başar, Pfluegers Arch. **405**, R45 (1985).
[28] P.E. Rapp, I.D. Zimmerman, A.M. Albano, G.C. deGuzman, and N.N. Greenbaun, Phys. Lett. **110A**, 335 (1985).
[29] P.E. Rapp, I.D. Zimmerman, A.M. Albano, G.C. deGuzman, N.N. Greenbaun, and T.R. Bashore, in *Nonlinear Oscillations in Biology and Chemistry*, edited by H.G. Othmer (Springer, Berlin, 1986), pp. 175–205.
[30] W.J. Freeman, Biol. Cybern. **56**, 139 (1987).
[31] C.A. Skarda and W.J. Freeman, Behav. Brain Sci. **10**, 161 (1987).
[32] I. Tsuda, E. Koerner, and H. Shimizu, Prog. Theor. Phys. **78**, 51 (1987).
[33] C. Chong Chen, Phys. Lett. A **213**, 148 (1995).
[34] Z. Zeng, W.C. Schieve, and P.K. Das, Physica D **67**, 224 (1993).
[35] K.-H. Kwek and J. Li, Neural, Parallel, & Scientific Computations **3**, 189 (1995).
[36] R.D. Beer, Adaptive Behavior **3**, 469 (1995).
[37] K.S. Cole and R.F. Baker, J. Gen. Physiol. **24**, 771 (1941).
[38] A.L. Hodgkin and A.F. Huxley, J. Physiol. **117**, 500 (1952).
[39] P.B. Detwiler, A.L. Hodgkin, and P.A. McNaughton, J. Physiol. **300**, 213 (1980).
[40] D.W. Wheeler, Ph.D. thesis, The University of Texas, 1998 (unpublished).
[41] W.J. Freeman, H.-J. Chang, B.C. Burke, P.A. Rose, and J. Badler, IEEE Trans. Circuits Syst. **44**, 989 (1997).
[42] S. Rajasekar and M. Lakshmanan, Physica D **67**, 282 (1993).
[43] L. Wang, IEEE Trans. Neural Networks **7**, 1382 (1996).
[44] A. Wolf, J.B. Swift, H.L. Swinney, and J.A. Vastano, Physica D **16**, 285 (1985).
[45] W.H. Press, S.A. Teukolsky, W.T. Vetterling, and B.P. Flannery, *Numerical Recipes in C: The Art of Scientific Computing* (Cambridge University Press, Cambridge, 1992).
[46] G.N. Milshtein, Theor. Probab. Appl. **23**, 396 (1978).
[47] L.M. Pecora and T.L. Carroll, Phys. Rev. Lett. **64**, 821 (1990).
[48] L.M. Pecora and T.L. Carroll, Phys. Rev. A **44**, 2374 (1991).
[49] R. Toral, C.R. Mirasso, E. Hernández-García, and O. Piro, Chaos **11**, 665 (2001).